The Plant Cell, Vol. 11, 1609–1621, September 1999, www.plantcell.org © 1999 American Society of Plant Physiologists

RESEARCH ARTICLE

The Phosphoenolpyruvate/Phosphate Translocator Is Required for Phenolic Metabolism, Palisade Cell Development, and Plastid-Dependent Nuclear Gene Expression

Stephen J. Streatfield,[a,b,1] Andreas Weber,[c] Elizabeth A. Kinsman,[d] Rainer E. Häusler,[c] Jianming Li,[a] Dusty Post-Beittenmiller,[b] Werner M. Kaiser,[e] Kevin A. Pyke,[d] Ulf-Ingo Flügge,[c] and Joanne Chory[a,f,2]

[a] Plant Biology Laboratory, Salk Institute for Biological Studies, La Jolla, California 92037
[b] Plant Biology Division, Samuel Roberts Noble Foundation, Ardmore, Oklahoma 73402
[c] Botanisches Institut der Universität zu Köln, Lehrstuhl II, Gyrhofstrasse 15, D-50931 Cologne, Germany
[d] School of Biological Sciences, Royal Holloway University of London, Egham, Surrey TW20 0EX, United Kingdom
[e] Julius-von-Sachs-Institute for Biosciences, Julius-von-Sachs-Platz 2, 97082 Wuerzburg, Germany
[f] Howard Hughes Medical Institute Research Laboratories, La Jolla, California 92037

The Arabidopsis *chlorophyll a/b binding protein* (*CAB*) *gene underexpressed 1* (*cue1*) mutant underexpresses light-regulated nuclear genes encoding chloroplast-localized proteins. *cue1* also exhibits mesophyll-specific chloroplast and cellular defects, resulting in reticulate leaves. Both the gene underexpression and the leaf cell morphology phenotypes are dependent on light intensity. In this study, we determine that *CUE1* encodes the plastid inner envelope phosphoenolpyruvate/phosphate translocator (PPT) and define amino acid residues that are critical for translocator function. The biosynthesis of aromatics is compromised in *cue1*, and the reticulate phenotype can be rescued by feeding aromatic amino acids. Determining that *CUE1* encodes PPT indicates the in vivo role of the translocator in metabolic partitioning and reveals a mesophyll cell–specific requirement for the translocator in Arabidopsis leaves. The nuclear gene expression defects in *cue1* suggest that a light intensity–dependent interorganellar signal is modulated through metabolites dependent on a plastid supply of phosphoenolpyruvate.

INTRODUCTION

The global control of cellular metabolism is achieved in part through the compartmentalization of metabolic pathways between organelles. However, compartmentalization necessitates the transport of particular key metabolites across membranes of limited permeability. The inner envelope membrane of plastids is the key site for the transport of metabolic intermediates between the plastid stroma and the cytoplasm. Five metabolite translocators have been identified in the plastid inner envelope. The triose phosphate/phosphate translocator (TPT) exports fixed photosynthate from chloroplasts (Flügge et al., 1989; Loddenkötter et al., 1993). The 2-oxoglutarate/malate translocator facilitates nitrogen assimilation into chloroplasts (Weber et al., 1995). The ATP/ADP translocator provides the plastid with ATP (Neuhaus et al., 1997). The phosphoenolpyruvate/phosphate translocator (PPT) imports phosphoenolpyruvate (PEP) into plastids (Fischer et al., 1997), and the glucose 6-phosphate/phosphate translocator (GPT) imports glucose 6-phosphate into plastids for starch biosynthesis and for the oxidative pentose phosphate pathway (Kammerer et al., 1998). In each case, the designation of substrate specificity, and thus of proposed metabolic function, has depended on experiments investigating the in vitro transport specificity of the heterologously expressed translocator in an artificial membrane system.

In the case of PPT, a cDNA was initially isolated on the basis of the phosphate translocation activity of the encoded protein (Fischer et al., 1997). The plastid localization of PPT is implied by a putative N-terminal targeting sequence and by the import of in vitro–synthesized PPT into the envelope fraction of isolated plastids (Fischer et al., 1997). Moreover, hydrophobicity distribution analysis of the mature protein predicts six transmembrane domains. A proposed role for PPT is to provide PEP for the synthesis of aromatic amino acids and related compounds through the shikimate pathway. The identification of mutants with deficient translocators would

[1] Current address: Prodi Gene, Inc., 101 Gateway Blvd., College Station, TX 77845.
[2] To whom correspondence should be addressed at the Howard Hughes Medical Institute/Plant Biology Laboratory, Salk Institute, 10010 N. Torrey Pines Rd., La Jolla, CA 92037. E-mail chory@salk.edu; fax 858-558-6379.

allow the postulated roles of the translocators to be ascertained in vivo and the physiological importance of metabolite partitioning to be assessed.

Here, we identify the *CHLOROPHYLL a/b BINDING PROTEIN* (*CAB*) *GENE UNDEREXPRESSED 1* (*CUE1*) gene of Arabidopsis and determine that it encodes PPT. The *cue1* mutant was isolated from a genetic screen based on the aberrant expression of *CAB* (Li et al., 1995), and *cue1* underexpresses several plastid and nuclear genes encoding plastid-localized proteins. The chlorophyll and carotenoid components of the light-harvesting and photoprotective machinery are also diminished in *cue1*. In addition, *cue1* has a reticulate phenotype in which interveinal regions of the leaves are visibly pale, whereas paraveinal regions are green. This visible phenotype extends to the ultrastructural level. Mesophyll cells and chloroplasts appear aberrant in *cue1*, whereas bundle sheath cells and chloroplasts appear like the wild type. Furthermore, plants carrying severe alleles of *cue1* require an exogenous carbon source before they can establish photoautotrophic growth, and they only accumulate approximately one-third of the biomass of the wild type (Li et al., 1995).

The demonstration that *CUE1* encodes PPT has allowed us to identify amino acid residues required for PPT function and to assess metabolic and photosynthetic deficiencies in a translocator-deficient background. In addition, we demonstrate that the morphological and gene underexpression phenotypes of *cue1* are light intensity dependent. This study emphasizes the metabolic routing of PEP into the shikimate pathway after translocation by PPT and demonstrates the importance of PPT for mesophyll cell development and for the expression of nuclear genes encoding plastid components.

RESULTS

cue1 Has a Gene Underexpression Phenotype and a Mesophyll Cell–Specific Leaf Morphology Defect

Two alleles of the *cue1* mutant of Arabidopsis (*cue1-1* and *cue1-3*) were isolated through a selectable marker–based screen in which survival depended on reduced expression of an alcohol dehydrogenase (*ADH*) gene driven by the *CAB3* promoter (Li et al., 1995; López-Juez et al., 1998). However, in addition to their gene expression phenotype, these alleles also have a reticulate leaf phenotype, and we have now identified six additional *cue1* alleles (*cue1-2* and *cue1-4* through *cue1-8*) on the basis of this visible phenotype (Figure 1A). The reticulate pattern is evident in cotyledons, rosette leaves, and cauline leaves and is most obvious when leaves are young and expanding, because older, fully expanded leaves tend to turn darker green (Figure 1B). We compared *CAB* mRNA levels in the six new alleles with those of the two old alleles (*cue1-1* and *cue1-3*). At 14 days

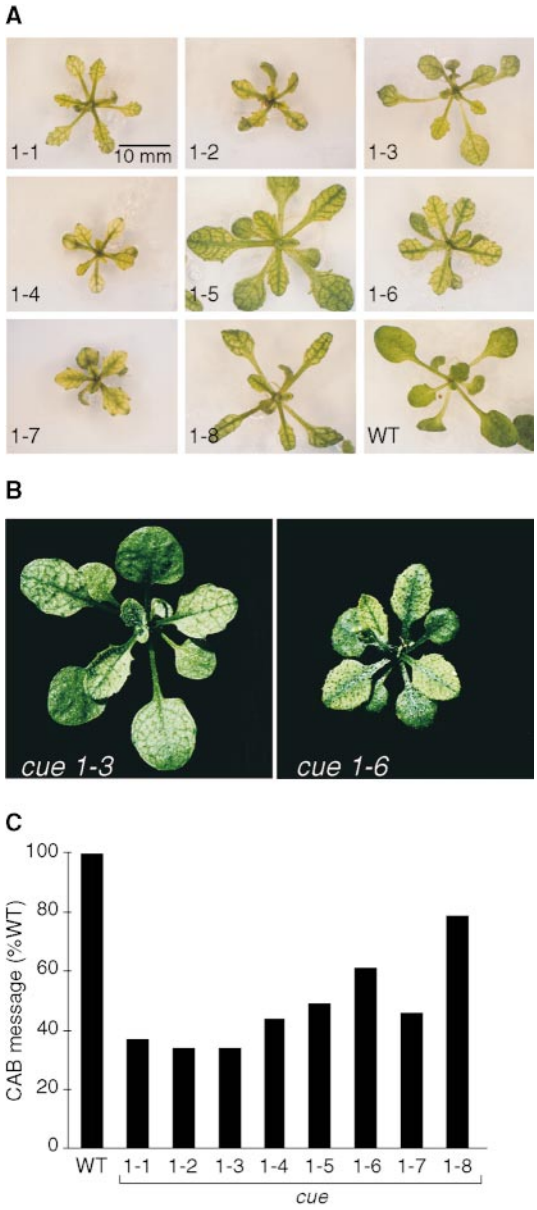

Figure 1. Multiple Alleles of *cue1* Have a Reticulate Leaf Phenotype and a *CAB* Underexpression Phenotype.

(A) Seedlings were grown in tissue culture for 17 days under a 16-hr-light and 8-hr-dark photoperiod with a photon flux density of 200 μmol m^{-2} sec^{-1} of white light.
(B) Plants carrying the weak *cue1-3* and strong *cue1-6* alleles were grown for 29 days under a 16-hr-light and 8-hr-dark photoperiod.
(C) *CAB* message levels were determined by RNA gel blot hybridization and normalized to 18S rRNA. RNA was prepared from seedlings grown in tissue culture for 14 days under a 16-hr-light and 8-hr-dark photoperiod with a photon flux density of 200 μmol m^{-2} sec^{-1} of white light. Tissue was harvested 6 hr into the light period.
WT, wild type.

of growth, the levels range from 34 to 79% of that of the wild type (Figure 1C), demonstrating that *CAB* underexpression is a consistent aspect of the phenotype. As with the reticulate leaf phenotype, the *cue1* defect in *CAB* expression is most evident early in development, with a strong allele having only ~25% of wild-type expression at 3 days after germination but ~50% at 15 days (Li et al., 1995).

The basis of the reticulate phenotype of *cue1* is evident from leaf morphology. The proportion of leaf transect area occupied by air is much greater in *cue1* than in the wild type (Table 1). An analysis of the proportion of each cell type in leaves demonstrates that this increased airspace is primarily a result of a reduction in the number of palisade mesophyll cells (Table 1). By contrast, the proportions of spongy mesophyll and epidermal cells are not affected, and the proportion of bundle sheath cells is increased. There is no consistent reduction in the size of either mesophyll or bundle sheath cells in *cue1* (data not shown). There is also a mesophyll cell–specific plastid phenotype in *cue1*. Mesophyll cells in fourth leaves of *cue1* have smaller chloroplasts than in corresponding wild-type cells (Table 2). By contrast, bundle sheath cell chloroplasts in fourth leaves of *cue1* are indistinguishable from those of the wild type (Table 2). There is no reduction in plastid number per cell for either cell type (data not shown).

Table 2. Plastid Plan Area in *cue1* and Wild-Type Leaves

	Plastid Plan Area (μm^2)[a]	
Genotype	Mesophyll Cells	Bundle Sheath Cells
pOCA108	34.0	19.8
cue1-1	19.7	22.9
cue1-3	28.0	21.9
Columbia	30.4	21.8
cue1-2	23.9	21.9
cue1-5	26.4	19.7

[a] Values are means of data for 194 to 630 chloroplasts per sample. Standard errors of the means are in all cases <4% of the means.

Photosynthetic Parameters Are Affected in *cue1*

The *cue1* mutant is severely compromised in establishing photoautotrophic growth. We examined the physiological basis for this defect by monitoring photosynthetic electron transport and measuring the variable fluorescence/maximum fluorescence (F_v/F_m) ratio of dark-adapted leaves, which gives a measure of excitation energy transfer in intact photosystem II reaction centers. Plants carrying the *cue1-3* and *cue1-1* alleles have, respectively, moderate and severe reductions in the photosynthetic electron transport rate at steady state, correlating with the relative strengths of the reduced growth phenotype (Figure 2A). However, the induction kinetics of photosynthetic electron transport are similar in *cue1-1* and *cue1-3* compared with the control strain (Figure 2A). There is a minor effect on the F_v/F_m ratio, which is reduced to 90% of that of the wild type in plants carrying the strong *cue1-1* allele (data not shown).

The time course of chlorophyll *a* quenching, monitored by measuring the photochemical quenching coefficient (q_P) and the nonphotochemical quenching coefficient (q_N), is also altered in *cue1-1*. The value of q_P gives information on the redox state of the primary quinone redox acceptor in photosystem II (Q_A), such that $Q_{A(reduced)}\% = (1 - q_P) \times 100$. At intermediate light intensities, the major part of q_N correlates with the transthylakoid proton gradient, $q_N = q_{NE}$ (Krause and Weis, 1991). Thus, whenever the linear electron flow from photosystem II to photosystem I is disrupted, Q_A becomes more reduced (q_P declines). If this decrease in electron flow is coupled with the generation of the pH gradient across the thylakoid membrane, q_N (q_{NE}) also declines. The induction of both q_P and q_N is markedly slower in *cue1-1* than in the wild type (Figures 2B and 2C), showing that the electron flux and the generation of the pH gradient are impaired

Table 1. Proportion of Airspace[a] and Proportion of Each Cell Type[b] in *cue1* and Wild-Type Leaves[c]

Genotype[d]	Airspace (%)	Palisade Mesophyll (%)	Spongy Mesophyll (%)	Bundle Sheath (%)	Epidermis (%)	pal/ccc[e] (%)
pOCA108	16.9	17.7	34.3	9.3	38.7	28.9
cue1-1	25.8	10.3	34.2	14.4	41.1	17.4
cue1-3	30.6	10.8	35.0	14.3	40.9	18.0
Columbia	16.8	16.9	37.6	8.3	37.2	26.9
cue1-2	31.0	11.7	38.4	9.1	40.9	19.9
cue1-5	27.7	12.8	32.5	12.3	42.3	22.3

[a] Proportion of half leaf transect area occupied by airspace in fully expanded fourth leaves.
[b] Transects through each type of cell as a proportion of total transects through cells.
[c] Values are means of data for three leaves. Standard errors of the means are in all cases <19% of the means.
[d] In the pOCA108 background, *cue1-1* and *cue1-3* are strong and weak alleles, respectively, whereas in the Columbia background, *cue1-2* and *cue1-5* are strong and weak alleles, respectively.
[e] Palisade (pal) cells as a proportion of total chloroplast-containing cells (ccc; palisade + spongy mesophyll + bundle sheath).

in *cue1*. However, under steady state conditions, q_P and q_N are similar in *cue1* and the wild type (data not shown), indicating that the redox state of Q_A as well as the transthylakoid proton gradient can adapt to the decline in the rate of photosynthetic electron transport in *cue1-1*.

The Reticulate Leaf and *CAB* Underexpression Phenotypes of *cue1* Are Light Intensity Dependent

The reticulate phenotype of *cue1* is clearest when seedlings are grown under light at high fluence rates. In dim light conditions, *cue1* seedlings show little or no paleness (Figure 3A). The extent of the *CAB* underexpression phenotype is also dependent on light intensity. Whereas dark-grown *cue1* seedlings have a basal level of *CAB* mRNA that is similar to that of the wild type (Figure 3C), light-grown *cue1* seedlings underexpress *CAB*, and this underexpression is more apparent at a higher light intensity (Figure 3B). At a low light intensity, *CAB* mRNA levels in plants carrying the weak *cue1-5* and strong *cue1-2* alleles are 69 and 49% of that of the wild type, respectively, whereas at a higher light intensity, the corresponding levels are 41 and 35% of that of the wild type.

The light intensity dependence of the *CAB* underexpression phenotype is also evident when etiolated seedlings are treated with a pulse of light. The *cue1* mutant has a reduced capacity to respond to a light pulse, and this reduced response is clearer at a high fluence (Figure 3C). In *cue1*, *CAB* induction with a low-fluence red light pulse is 27% lower than that with a high-fluence white light pulse. By contrast, with the wild type, a high-fluence pulse induces *CAB* by only 11% less than does a low-fluence pulse.

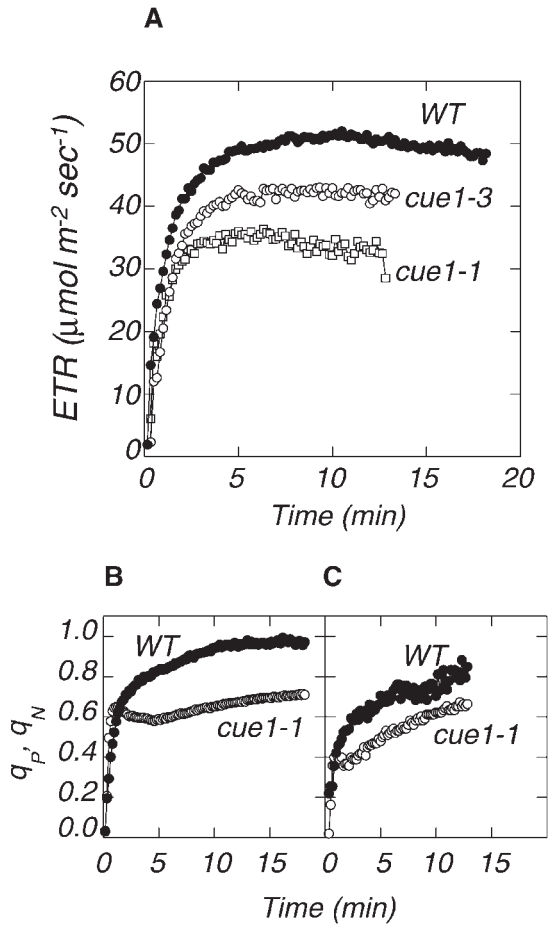

Figure 2. Photosynthetic Parameters Are Affected in *cue1* Compared with pOCA108 (WT).

(A) Typical induction kinetics of photosynthetic electron transport (ETR).

(B) Time course of photochemical (q_P) chlorophyll *a* quenching.

(C) Time course of nonphotochemical ($q_N = q_{NE}$) chlorophyll *a* quenching.

CUE1 Corresponds to the Plastid Inner Envelope Protein PPT

A seedling with a *cue1*-like reticulate leaf morphology was identified in a collection of T-DNA–tagged lines (generated by I. Kardailsky and D. Weigel, unpublished results). This reticulate mutant is recessive and allelic to *cue1* and was designated *cue1-8*. In a backcross, a T-DNA–derived polymerase chain reaction (PCR) marker cosegregated with the reticulate phenotype. Left border T-DNA sequence was used to probe *cue1-8* DNA, and it identified a fragment reduced in size from 2.5 kb in a HindIII digest to 1.2 kb in a HindIII/EcoRI double digest (Figure 4A). Genomic sequences flanking the left border were obtained by using the thermal asymmetric interlaced (TAIL) PCR procedure. One of the subcloned products of these reactions hybridizes strongly to a single HindIII DNA fragment that shifts in size between *cue1-8* and the wild type (Figure 4B). As predicted, this fragment is ~2.5 kb in *cue1-8*. The nucleotide sequence of the subcloned PCR product was determined (Figure 4C). The T-DNA left border sequence is flanked by 28 nucleotides of new sequence and then with sequence that is 100% identical to the Arabidopsis plastidic *PPT* (Fischer et al., 1997).

CUE1 was confirmed as corresponding to *PPT* by identifying mutations at the *PPT* locus in all eight alleles of *cue1* (Figure 5A and Table 3). *PPT* is deleted in *cue1-1* and *cue1-2* and is disrupted in *cue1-8* (Figure 5A). In addition to the *PPT* locus, a *PPT* sequence probe also identifies at least two other DNA fragments (Figure 5A). These do not correspond to the related *TPT*, because a *TPT* sequence probe identifies another distinct locus (Figure 5B). Thus, additional translocators, more closely related to PPT than to TPT, are likely to be present in Arabidopsis.

Further evidence demonstrating that *CUE1* is *PPT* was obtained by analyzing the *PPT* message all eight *cue1* alleles

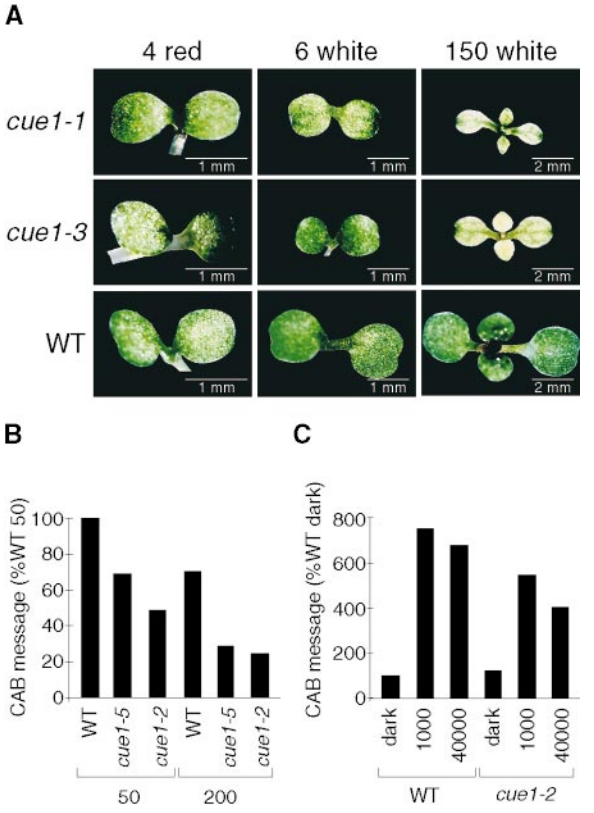

Figure 3. The Reticulate and *CAB* Underexpression Phenotypes of *cue1* Are Dependent on Light Intensity.

(A) Mutants carrying the strong *cue1-1* and weak *cue1-3* alleles and the wild type (pOCA108) were grown in tissue culture for 7 days under constant red light (600-nm filter) at a photon flux density of 4 μmol m^{-2} sec^{-1} or white light at a photon flux density of 6 or 150 μmol m^{-2} sec^{-1}, as indicated above the panels.

(B) *CAB* message levels were determined by RNA gel blot hybridization and normalized to levels of 18S rRNA. RNA was prepared from the wild-type (Columbia) and *cue1* seedlings that had been grown in tissue culture for 13 days under constant white light at photon flux densities of 50 or 200 μmol m^{-2} sec^{-1}. %WT 50 represents *CAB* message levels as a percentage of the level in the wild type at a photon flux density of 50 μmol m^{-2} sec^{-1}.

(C) *CAB* message levels were determined by RNA gel blot hybridization and normalized to levels of 18S rRNA. Seeds were exposed to a photon flux density of 200 μmol m^{-2} sec^{-1} of white light for 1 hr and grown in the dark for 6 days. Etiolated seedlings were left in the dark or given light pulses of 1000 μmol m^{-2} (33 μmol m^{-2} sec^{-1} for 30 sec) red light (650-nm filter) or 40,000 μmol m^{-2} (267 μmol m^{-2} sec^{-1} for 150 sec) white light, using a 100-W quartz tungsten halogen fiber optic light source. Seedlings were then returned to the dark for 4 hr before tissue was harvested for RNA preparation.

WT, wild type.

(Figure 5C). The *PPT* probe identifies a single message in the wild type, and this is absent from *cue1-1*, *cue1-2*, *cue1-6*, and *cue1-8*. An extended exposure identifies a much less abundant message in *cue1-8* that is ~0.3 kb smaller than the wild-type message (Figure 5D). In addition, the reticulate leaf phenotype of *cue1-6* is completely rescued by transformation with cauliflower PPT cDNA (data not shown).

In cauliflower and maize, *PPT* is expressed at a low level in all tissues (Fischer et al., 1997; Kammerer et al., 1998). *PPT* message level in Arabidopsis is also at a low but uniform level (Figure 5E). As with other species, *TPT* is more strongly expressed than *PPT*, but *TPT* message level in roots is relatively low (Figure 5E).

cue1 Has Reduced Levels of Key Aromatic Metabolites and Can Be Rescued by Feeding Aromatic Amino Acids

To examine the metabolic routing of PEP once imported into plastids, we investigated the levels of various key metabolites in *cue1*. The principal fate of imported PEP is proposed to be the shikimate pathway. Indeed, secondary products that are dependent on the shikimate pathway for precursors are clearly reduced in *cue1*. Under long-wavelength UV light, *cue1-1* glows orange (Figure 6A), which is indicative of chlorophyll fluorescence in the absence of phenolic compounds to absorb UV light (Chapple et al., 1992). HPLC analysis indicates reduced flavonoids (57%), hydroxycinnamic acids (63.5%), and simple phenolics (84%) in *cue1-1* when compared with the wild type. Furthermore, when grown under high light stress conditions, both the strong *cue1-1* and weak *cue1-3* alleles show a reduced capacity to induce anthocyanins (Figure 6B). This reduced anthocyanin production is also evident in leaf tissue when seedlings are shifted from a low to a high fluence rate (Figures 6C and 6D).

The overall level of free amino acids is higher in *cue1-1* (14.5 μmol g^{-1} fresh weight) than in the wild type (9.16 μmol g^{-1} fresh weight), and the ratio of nonaromatic to aromatic amino acids is also higher in *cue1-1* (362.5) than it is in the wild type (152.6). This indicates an imbalance between the metabolism of aromatic and nonaromatic amino acids. In particular, arginine is 10-fold higher in *cue1-1* than in the wild type (Table 4). There is also a two- to threefold increase in urea in *cue1-1*, which might be due to an increase in amino acid catabolism.

The best evidence that the primary metabolic defect in *cue1* is a reduced flux through the shikimate pathway is that the reticulate leaf phenotype of *cue1-1* can be rescued by feeding with all three aromatic amino acids together (Figure 7), although not with any one aromatic amino acid alone (data not shown). Although another possible fate for PEP imported into plastids is to be channeled through pyruvate into fatty acid biosynthesis, overall lipid levels are unaffected in *cue1* leaves and seeds (data not shown), indicating that there is not a major flux of PEP into this pathway.

We also compared the levels of starch and soluble sugars

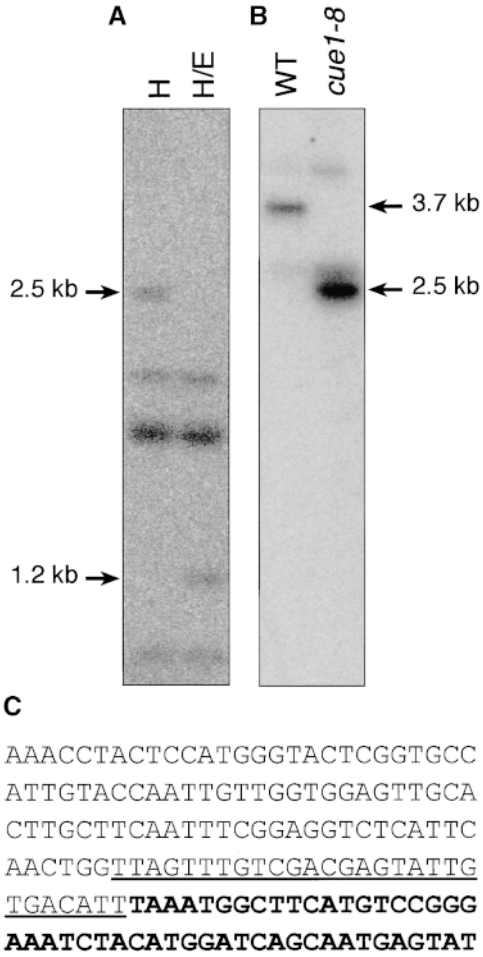

Figure 4. The *CUE1* Locus in the Tagged Allele, *cue1-8*.

(A) DNA gel blot hybridization, using a T-DNA left border sequence probe, of HindIII (H) versus HindIII/EcoRI (H/E) digests of *cue1-8* DNA. The indicated bands identify fragments unique to a restriction enzyme digest.

(B) DNA gel blot hybridization, using the subcloned TAIL-PCR product (obtained with primer AD1) as probe for HindIII digests of Columbia (WT) and *cue1-8* DNA. The indicated bands identify the *CUE1* locus in the wild type and *cue1-8*.

(C) DNA sequence at the left border of the T-DNA insertion site of *cue1-8* showing the *PPT* sequence, new sequence (underlined), and T-DNA sequence (boldface type).

between *cue1-1* and the wild type. Although there is little difference in the total amount of starch that accumulates during the day, marked differences are evident in the accumulation of soluble sugars (Table 5). In *cue1-1*, the concentrations of soluble sugars are substantially lower than in the wild type, and unlike the wild type, there is very little diurnal variation. There is clearly an imbalance between carbohydrate and nitrogen metabolism in *cue1*. Whereas levels of urea and the amino acids glutamine, asparagine, and arginine are elevated in *cue1* (Table 4), and there is also a three- to fourfold increase in the level of nitrate (data not shown), the levels of soluble sugars are reduced (Table 5).

The concentrations of a range of anions were also determined in *cue1-1* and the wild type (data not shown). By far the most significant difference was observed with phosphate, which is present in *cue1-1* at only 6% of the level found in the wild type.

The Rapid Induction Kinetics of Chlorophyll *a* Imply a Reduced Plastoquinone Pool Size in *cue1*

A key photosynthetic electron carrier, plastoquinone, is dependent on the shikimate pathway for its synthesis, and flux through this pathway is likely to be limiting in *cue1*. Therefore, we attempted to assess the relative pool size of plastoquinone in vivo by monitoring the rapid induction kinetics of chlorophyll *a* fluorescence in *cue1* alleles versus the wild type. The induction of chlorophyll *a* fluorescence upon illumination of a dark-adapted leaf is multiphasic. The first rapid increase from ground fluorescence (F_o) to fluorescence at the inflection point (F_i) is due to the reduction of a population of the primary quinone redox acceptor in photosystem II, Q_A, that is not associated with the plastoquinone pool. The slower increase to maximum fluorescence at nonsaturating light (F_p), equivalent to maximum fluorescence at saturating light (F_m), is based on the reduction of the plastoquinone pool via Q_A (Horton and Bowyer, 1990). The additional slower changes in fluorescence yield in a second-to-minute scale are principally due to biochemical limitations of the Calvin cycle.

The relative pool sizes of plastoquinone, determined from the area under the fluorescence induction curves in the absence of nonassociated Q_A, are lowered to a similar degree of 10 to 50% in plants carrying the strong alleles *cue1-1* and *cue1-6* compared with the wild type (Figure 8). Moreover, the ratio of the plastoquinone pool to Q_A molecules not associated with soluble plastoquinones is decreased from 85 ± 15 ($n = 5$) in the wild type to 52 ± 14 ($n = 6$) in *cue1-1* and *cue1-6*, these alleles being indistinguishable from each other. These data suggest that in *cue1*, the size of the plastoquinone pool may be reduced, and thus a higher proportion of Q_A is not associated with soluble plastoquinone molecules in the thylakoid membrane.

DISCUSSION

The localization of metabolic pathways within organelles necessitates the partitioning of key metabolites. This partitioning requires the translocation of metabolites across organellar membranes. In plant cells, several metabolic pathways are unique to plastids, and the inner envelope membrane of

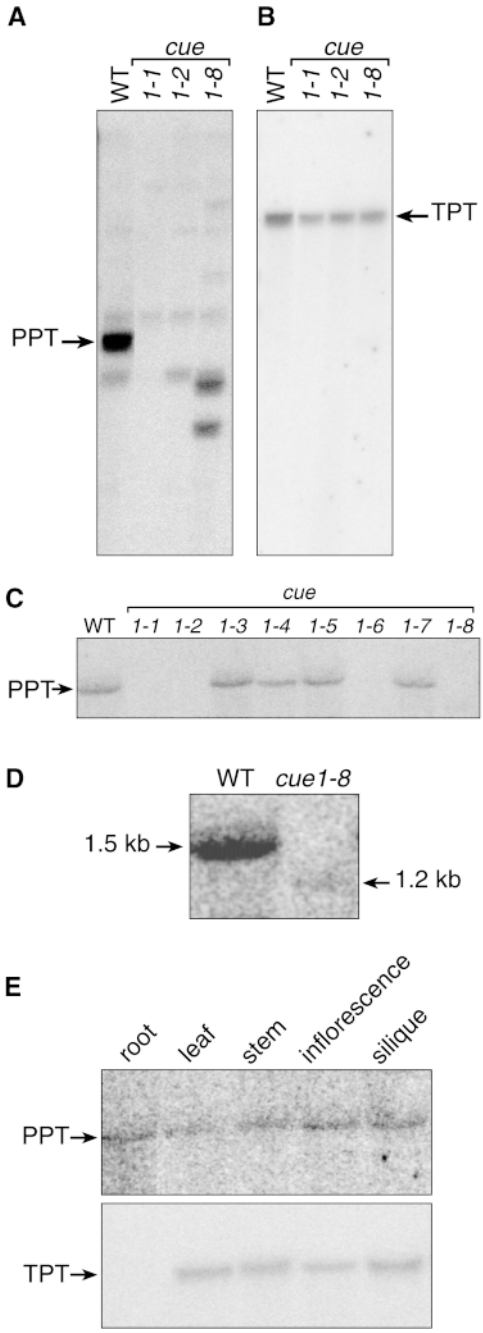

Figure 5. The *cue1* Locus Corresponds to *PPT*, Which Is Expressed Ubiquitously and at a Low Level.

(A) DNA gel blot hybridization, using a *PPT* sequence probe, of HindIII digests of Arabidopsis DNA.

(B) DNA gel blot hybridization, using a *TPT* sequence probe, of HindIII digests of Arabidopsis DNA.

(C) RNA gel blot hybridization, using a *PPT* sequence probe, of RNA prepared from seedlings grown in tissue culture for 7 days under a 16-hr-light and 8-hr-dark photoperiod with a photon flux density of 200 μmol m^{-2} sec^{-1} of white light. Tissue was harvested 6 hr into the light period.

(D) As given for **(C)**, but at a fourfold longer exposure. The indicated 1.5-kb message corresponds to wild-type *PPT*, and the indicated 1.2-kb message corresponds to a possible truncated *PPT* transcript in *cue1-8*.

(E) RNA gel blot hybridization, using *PPT* and *TPT* sequence probes, of RNA prepared from different tissues of wild-type ecotype Columbia. The exposure for the *PPT* hybridizing signal is ~20 times that for the *TPT* signal.

WT, wild type.

plastids largely isolates these pathways from cytosolic metabolism. However, key metabolic intermediates are transported across the inner envelope membrane by translocators of defined specificity. Here, we demonstrate that the *cue1* mutant of Arabidopsis is deficient in PPT, the plastid translocator of PEP. The analysis of multiple alleles of *cue1* defines critical amino acid residues for translocator activity and has allowed us to assess the metabolic and broader physiological consequences of disrupting the partitioning of PEP.

Multiple *cue1* Alleles Identify Critical Residues for PPT Activity

Three alleles of *cue1* identify Gly-167, Arg-181, and Ala-304 as being important for function. These residues are conserved in PPT from Arabidopsis, cauliflower, tobacco, and maize (Fischer et al., 1997) and also in TPT (Flügge et al., 1989) and GPT (Kammerer et al., 1998). Gly-167 and Arg-181 lie between putative transmembrane spans III and IV, and Ala-304 lies within putative transmembrane span VI. Whereas Gly-167 and Ala-304 lie in regions of high sequence similarity between translocator types, Arg-181 lies in an otherwise divergent region. The conservation of these amino acids between translocators with different metabolite preferences indicates that they are important for basic translocator structure and function rather than for determining substrate specificity.

Reduced Phenolic Levels in *cue1* Indicate That Translocated PEP Feeds Principally into the Shikimate Pathway

When reconstituted into artificial membranes, PPT preferentially translocates PEP in exchange for inorganic phosphate (Fischer et al., 1997). The requirement for a PEP translocator in the plastid inner envelope was proposed because PEP is a necessary substrate for the shikimate pathway, which is plastid localized (Schmid and Amrhein, 1995). Most plastids have little or no phosphoglycerate mutase or enolase activity (Bagge and Larsson, 1986), and PEP is a poor substrate for other known plastid translocators (Kammerer et al., 1998), thus necessitating a specific PEP translocator. The shikimate pathway provides aromatic amino acids for protein

synthesis and should be particularly important early in development. In correlation with a more important early role for PPT, the reticulate leaf and *CAB* underexpression phenotypes and the requirement for an exogenous carbon supply are most pronounced in young *cue1* seedlings.

Although there is not a major decrease in the levels of aromatic amino acids in the *cue1* mutant, the ratio of nonaromatic to aromatic amino acids is higher in *cue1* than in the wild type. There is also a reduction in the levels of phenolic compounds derived from shikimate pathway products, including hydroxycinnamic acids and anthocyanins. This aspect of the phenotype is similar to the *sinapoyl malate biosynthesis1* (*sin1*) mutant of Arabidopsis and to Antirrhinum lines overexpressing either of two *MYB* genes (Chapple et al., 1992; Tamagnone et al., 1998a, 1998b). The metabolic rescue of *cue1* by pooled aromatic amino acids further indicates that reduced flux through the shikimate pathway is the primary metabolic defect.

Tobacco plants overexpressing the transcription factor encoded by the *AmMYB308* gene from Antirrhinum are also impaired in phenolic acid metabolism and monolignol biosynthesis (Tamagnone et al., 1998a). Like *cue1*, these transgenic tobacco plants exhibit a reticulate phenotype. The identical phenotypes observed in transgenic tobacco and in the *cue1* mutants point to the role of the shikimate pathway in establishing proper leaf morphology. A likely cause of the reticulate phenotype in tobacco is a deficiency in the production of active isomers of the growth factor dehydrodiconiferyl alcohol glucoside, a derivative of phenolic acid metabolism (Tamagnone et al., 1998b).

PEP may also feed through pyruvate into the plastidic pathway for isopentenyl biosynthesis (reviewed in Lichtenthaler et al., 1997). A deficiency in the translocation of PEP into the plastid should then result in reduced synthesis of carotenoids and the prenyl side chains of chlorophylls and plastoquinone. Indeed, at 5 days after germination, *cue1* has only one-third the level of carotenoids and one-quarter the level of chlorophylls that are found in the wild type (Li et al.,

Table 3. Mutations at the *PPT* Locus in the *cue1* Alleles

Allele	Mutagen	Allele Strength	Mutation
cue1-1	Gamma ray	Strong	Locus deleted
cue1-2	Fast neutron	Strong	Locus deleted
cue1-3	EMS[a]	Weak	Ala at 304 to Val
cue1-4	T-DNA; unlinked	Strong	C-terminal 25 aa[b] deletion
cue1-5	EMS	Weak	Arg at 181 to Cys
cue1-6	EMS	Strong	Trp at −31 to stop
cue1-7	EMS	Strong	Gly at 167 to Glu
cue1-8	T-DNA; linked	Weak	T-DNA insert at Trp165

[a] EMS, ethyl methanesulfonate.
[b] aa, amino acid.

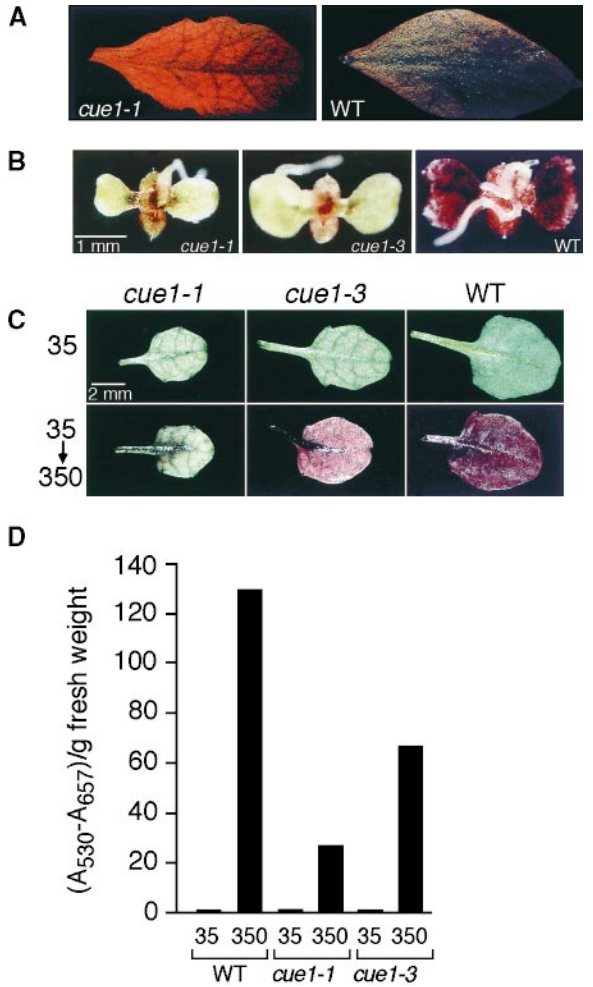

Figure 6. The Levels of Key Aromatic Metabolites Are Reduced in *cue1*.

(A) pOCA108 (WT) and *cue1-1* seedlings were grown in tissue culture for 26 days under constant light of a photon flux density of 35 μmol m^{-2} sec^{-1}, and the adaxial surfaces of rosette leaves were photographed under UV light.

(B) Seedlings were grown in tissue culture for 12 days under constant light of a photon flux density of 350 μmol m^{-2} sec^{-1} and photographed from below.

(C) Seedlings were grown in tissue culture for 12 days under constant light of a photon flux density of 35 μmol m^{-2} sec^{-1} and then either shifted to 350 μmol m^{-2} sec^{-1} or left at 35 μmol m^{-2} sec^{-1} for an additional 7 days. The abaxial surfaces of rosette leaves were photographed.

(D) Anthocyanin levels in leaves from seedlings grown as described in **(C)**.

1995). Quinone biosynthesis is dependent on the shikimate pathway supplying homogentisate and the plastidic pathway for isopentenyl biosynthesis supplying the associated prenyl side chain. Thus, quinone biosynthesis may be doubly affected in *cue1*. Reduced quinone levels may then also result in carotenoid defects, as in the *phytoene desaturation* (*pds1* and *pds2*) mutants of Arabidopsis, in which phytoene desaturation is blocked due to a deficiency in plastoquinone (Norris et al., 1995). The rapid induction kinetics of chlorophyll *a* fluorescence in *cue1* are consistent with a decrease in the size of the plastoquinone pool. However, further biochemical studies are required to verify an overall decline in plastoquinones.

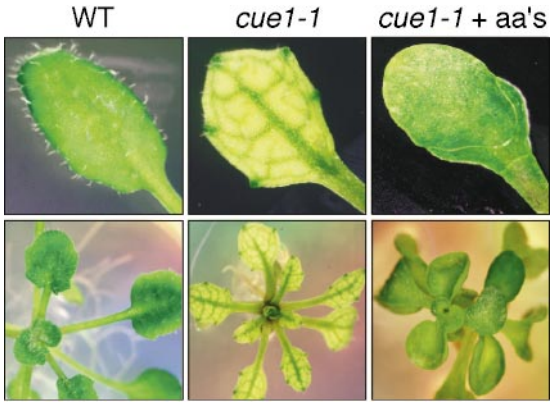

Figure 7. The Reticulate Leaf Phenotype of *cue1* Can Be Rescued by Feeding Aromatic Amino Acids.

Individual leaves (upper panels) and seedlings (lower panels) of *cue1-1* grown without or with added aromatic amino acids (aa's) and the wild type (WT; pOCA108) grown without added aromatic amino acids.

The Reticulate Phenotype of *cue1* Results from a Mesophyll Cell–Specific Defect

The reticulate leaf phenotype of *cue1* is shared by the *reticulata* (*re*) and *differential development of vascular-associated cells* (*dov*) mutants of Arabidopsis (Kinsman and Pyke, 1998). In *cue1*, this phenotype results from fewer palisade mesophyll cells, indicating a reduced rate of cell division in the mesophyll layer, and from aberrant mesophyll cell chloroplasts. By contrast, bundle sheath cell number and chloroplast size appear normal in *cue1*, and epidermal cells are also unaffected. The identification of *CUE1* as *PPT* indicates that within the leaf, PPT is required for normal cell division activity in the mesophyll cell layer of the young leaf primordium and for normal chloroplast development within this cell type. PPT appears to be particularly important in palisade cells; thus, *cue1* is similar to other mutants that are specifically affected in palisade cells. For example, the transposon-induced mutants *differentiation and greening* (*dag*) of Antirrhinum and *defective chloroplasts and leaves-mutable* (*dcl*) of tomato have sectors within which the palisade cells no longer have their characteristic columnar shape but adopt the spherical shape of spongy mesophyll cells, and the palisade cell chloroplasts have reduced granal stacking (Chatterjee et al., 1996; Keddie et al., 1996). The palisade layer is also disrupted in lines expressing the Arabidopsis homeobox gene *Athb-1* fused to a heterologous transactivating domain (Aoyama et al., 1995) and in tobacco overexpressing the transcription factor AmMYB308 (Tamagnone et al., 1998b). A more detailed gene expression analysis is required to determine whether *PPT* is expressed in mesophyll cells but not in bundle sheath cells or whether *PPT* is uniformly expressed but is not required for bundle sheath cell development. DNA gel blot hybridization analysis indicates multiple *PPT*-related sequences in Arabidopsis, and these sequences may correspond to genes encoding proteins of similar function in different cell types.

Table 4. Levels of Amino Acids and Related Compounds in *cue1*[a]

Compound	*cue1-1*	pOCA108	*cue1-1*/pOCA108
Phosphoserine	0.07	0.09	0.77
Urea	2.34	0.86	2.72
Aspartate	1.31	1.58	0.83
Threonine	0.77	0.57	1.35
Serine	1.98	1.15	1.72
Asparagine	1.67	0.44	3.8
Glutamate	4.1	2.52	1.63
Glutamine	2.4	1.54	1.56
α-Aminoadipinic acid	0.22	0.09	2.22
Proline	ND[b]	ND	
Glycine	0.1	0.06	1.67
Alanine	1.14	0.51	2.24
Citrulline	0.25	ND	
Valine	0.18	0.19	0.95
Cystine	ND	ND	
Methionine	0.02	0.05	0.4
Cystathionine	ND	ND	
Isoleucine	0.09	0.1	0.9
Leucine	0.14	0.28	0.5
Tyrosine	0.03	0.03	1
Phenylalanine	0.01	0.03	0.33
γ-Aminobutyric acid	0.51	0.92	0.55
Ammonia	0.21	0.16	1.31
Lysine	0.06	0.1	0.6
Histidine	0.04	0.02	2
Tryptophan	ND	ND	
Arginine	0.49	0.05	9.8

[a] Values are expressed as micromoles per gram fresh weight and are means of two independent samples. Standard errors are in all cases <15% of the means.
[b] ND, not detected.

Table 5. Starch and Soluble Sugar Levels and Diurnal Fluctuations in *cue1*[a]

Genotype	Time after Lights On (hr)[b]	Starch	Glucose	Fructose	Sucrose
pOCA108	0	3.84	0.91	1.01	3.34
pOCA108	12	20.03	1.25	1.47	6.40
cue1-1	0	4.19	0.46	0.34	1.95
cue1-1	12	17.56	0.60	0.35	2.05

[a] Starch is represented as micromoles of glucose equivalents per gram fresh weight, and soluble sugars are given as micromoles per gram fresh weight. Values are means of three independent samples, and standard errors of the means are in all cases <10% of the means.

[b] Plants were grown on a 12-hr-light and 12-hr-dark photoperiod.

The *CAB* Underexpression Phenotype of *cue1* Implicates Plastids in Mediating Information on Light Intensity to the Nucleus

The reticulate leaf and *CAB* underexpression phenotypes of *cue1* are light intensity dependent. The phenotypes of several other mutants are similarly dependent on light intensity. The *Su*/*Su* mutant of tobacco has reduced *CAB* message, specifically when it is exposed to high light (Kawata and Cheung, 1990). Similarly, the visible phenotypes of mutants affected in chlorophyll or carotenoid synthesis are dependent on light intensity (Hudson et al., 1993; Wetzel et al., 1994). Thus, the light intensity–dependent phenotypes of *cue1* are consistent with PEP ultimately feeding into the synthesis of photosynthetic and light-protective components within chloroplasts. Furthermore, a reduced *CAB* induction phenotype is apparent when etiolated *cue1* seedlings are given a pulse of light, indicating that etioplasts, like chloroplasts, can mediate signals controlling nuclear gene expression. Similar to *CAB* expression in constant light, the reduced light induction of *CAB* in etiolated *cue1* seedlings is more evident with a higher intensity light pulse. The introduction of a series of *CAB2* promoter/*LUCIFERASE* reporter fusions into *cue1* indicates that the underexpression phenotype of *cue1* is mediated through multiple proximal promoter sequences, including the *CAB* upstream factor 1 (CUF-1) binding site (data not shown). The CUF-1 binding site is similar to G-boxes (Anderson et al., 1994), and, because in Arabidopsis plastid signals can be mediated by G-boxes (Puente et al., 1996), a reduced level of *CAB* transcription in *cue1* may result from an altered plastid signal mediated through CUF-1.

Biochemical and genetic approaches have identified probable components of plastid/nuclear signaling. In *Dunaliella salina*, light- or temperature-induced changes in the redox state of Q_A, the primary quinone redox acceptor in photosystem II, affect *CAB* message accumulation (Maxwell et al., 1995), and the use of photosynthetic electron transport inhibitors has demonstrated that in *D. tertiolecta*, *CAB* transcription is dependent on the redox state of the plastoquinone pool (Escoubas et al., 1995). In Arabidopsis, excess light stress affects the redox state of the plastoquinone pool, resulting in a hydrogen peroxide–mediated photooxidative burst that precedes increased expression of two cytosolic ascorbate peroxidase genes (Karpinski et al., 1997, 1999). In *cue1*, a greatly reduced induction of the photochemical quench coefficient demonstrates that Q_A is more reduced (transiently), and, when illuminated, an altered redox poise in *cue1* may affect *CAB* transcription. Furthermore, reduced phenolic levels in *cue1* may contribute to the light intensity–dependent underexpression of *CAB*. Tobacco plants overexpressing *AmMYB308* have reduced phenolic levels (Tamagnone et al., 1998a). These plants also have an increased sensitivity to reactive oxygen species after pathogen infection, presumably because of a deficiency in phenolic antioxidants (Tamagnone et al., 1998b). Information on environmental light intensity affects the redox state of plastids and is also mediated by hydrogen peroxide (Karpinski et al., 1997, 1999). Therefore, the reduced level of phenolics in *cue1* should make it more susceptible to light intensity–induced reductions in *CAB* expression.

In summary, the identification of *CUE1* as *PPT* verifies the metabolic routing of PEP into the shikimate pathway in plastids. The reticulate phenotype of *cue1*, reflecting abnormal palisade cell morphology, demonstrates a mesophyll cell–specific requirement for PPT within the leaf. Furthermore, the underexpression phenotype implicates signals emanating from plastids as modulating the expression of nuclear genes encoding plastid components. Increases in light intensity greatly accentuate both the reticulate leaf and *CAB* underexpression phenotypes of *cue1*, indicating the importance of metabolites dependent on a plastid supply of PEP in sensing and responding to changes in light intensity.

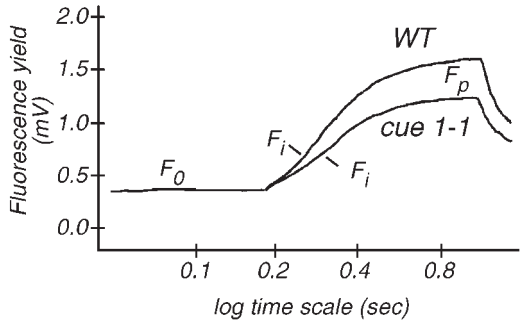

Figure 8. Typical Rapid Induction Kinetics of Chlorophyll *a* Fluorescence in *cue1* versus Wild Type (pOCA108).

Changes in chlorophyll *a* fluorescence are shown on a log time scale. The scale of fluorescence yield (arbitrary units; mV) is identical in both examples shown. F_o, F_i, and F_p are indicated. WT, wild type.

METHODS

Growth and Maintenance of *Arabidopsis thaliana*

The chlorophyll *a*/*b* binding protein (*CAB*) gene–underexpressing *cue1-1* and *cue1-3* alleles are in the Arabidopsis Bensheim ecotype transgenic background designated pOCA108, the *cue1-2* and *cue1-5* through *cue1-8* alleles are in the Columbia ecotype, and the *cue1-4* allele is in the C24 ecotype. The *cue1-5* and *cue1-6* alleles correspond to Arabidopsis Stock Center (Ohio State University, Columbus) lines CS3156 and CS3168, respectively. All *cue1* alleles were backcrossed to the relevant wild-type ecotype at least twice. To check for allelism, lines were crossed and the F_1 and F_2 progeny were scored for reticulate leaves. For tissue culture, seeds were surface sterilized, cold treated, and germinated on Murashige and Skoog medium (Murashige and Skoog salts, Gamborg's vitamins, 0.05% Mes, 1% sucrose, pH 5.7, and 0.8% phytagar). Seedlings were grown in chambers at 20°C under fluorescent and incandescent bulbs at the light fluence rate (photon flux density) and photoperiod conditions indicated. Plants were propagated on soil under greenhouse conditions.

Quantitation of mRNA Levels

Total RNA was isolated from plant tissues, as described by Chatterjee et al. (1996). RNA samples were size separated on agarose/formaldehyde gels, blotted onto nylon membranes, and hybridized to specific DNA probes. Filters were analyzed using a PhosphorImager (Molecular Dynamics, Sunnyvale, CA) and associated ImageQuant software.

Microscopic Analysis of Leaf Cells and Chloroplasts

Seedlings were grown under a 16-hr-light and 8-hr-dark photoperiod. Resin-embedded leaf sections and separated cell preparations were prepared and analyzed as described by Kinsman and Pyke (1998).

Measurement of Photosynthetic Electron Transport and Photochemical and Nonphotochemical Quenching

The quantum efficiency of electron flux through photosystem II was estimated according to Genty et al. (1989) and was used to calculate photosynthetic electron transport. F_v/F_m ratios were determined by applying saturated light pulses to 30-min dark-adapted leaves: pulses of photosynthetically active red light ($\lambda = 600$ nm) at a photon flux density of 240 μmol m^{-2} sec^{-1} were applied at 1-min intervals. Modulated chlorophyll *a* fluorescence emission from the upper surface of the leaf was measured using a pulse amplitude modulation fluorometer (PAM-2000; H. Walz, Effeltrich, Germany). Photochemical quenching (q_P) and nonphotochemical quenching (q_N) were determined according to Schreiber et al. (1986). The ground fluorescence (F_o) was measured by exposing leaves that had been dark-adapted for 30 to 60 min to a weak modulated measuring beam. For the determination of the maximum fluorescence (F_m), a flash of saturating light ($\sim$5000 μmol m^{-2} sec^{-1} of 800 msec duration) was applied. The variable fluorescence (F_v) was monitored after the onset of illumination with actinic light. For a more accurate determination of q_P and q_N, the quenching of F_o to F_o' (ground fluorescence in the dark, upon illumination) was determined by applying a 6-sec pulse of far red light in the absence of actinic illumination.

Isolation of the *PPT* Sequence

F_2 progeny of a backcross of the *cue1-8* allele were scored for the presence of the T-DNA insert by a polymerase chain reaction (PCR)–based assay. DNA was isolated from leaf tissue by a cetyltrimethylammonium bromide–based method, and DNA samples were size-separated on agarose gels, blotted onto nylon membranes, and hybridized with specific DNA probes. DNA gel blots were analyzed as given above for RNA gel blots. Genomic DNA flanking the T-DNA insertion site was isolated by thermal asymmetric interlaced (TAIL) PCR, according to the procedure of Liu et al. (1995). Potential genomic flanking sequences were subcloned into the pGEM-T vector (Promega), and their nucleotide sequence was determined. The phosphoenolpyruvate/phosphate translocator (*PPT*) locus was PCR amplified and sequenced in multiple ecotypes and *cue1* alleles by using combinations of primers derived from *PPT* cDNA sequence.

Pigment and Metabolite Analyses and Feeding Studies

Phenolic levels in leaves were visibly assessed by illuminating with UV light (366 nm), and photographs were taken using a yellow filter. For analysis of phenolic levels, 25 mg of freeze-dried tissue was ground to a fine powder and then extracted twice for 5 min at 4°C with 650 μL of 80% methanol and once with 650 μL of 50% methanol. The resulting suspensions were centrifuged for 10 min at 4°C, and the supernatants were pooled and analyzed by injecting 20 μL onto a Nucleosil 100-5 C8 column (Macherey-Nagel, Dueren, Germany) for HPLC. Solvents were A, 1% H_3PO_4, and B, 100% acetonitrile, and the gradient was 15 to 17% B for 8 min, 17% B for 5 min, 17 to 18% B for 3 min, 18 to 50% B for 10 min, 50 to 100% B for 1 min, 100% B for 4 min, 100 to 15% B for 1 min, and 15% B for 6 min.

For anthocyanin measurements, frozen tissue was ground up and incubated in 1% HCl in methanol for $\sim$16 hr. A 66% volume of water was added, and chlorophylls were then extracted with an equal volume of chloroform. Anthocyanins in the aqueous/methanol phase were quantified spectrophotometrically by determining $A_{530nm} - A_{657nm}$.

For anion and amino acid analyses, 0.5-g amounts of leaf material were frozen, ground, and resuspended in water (10 volumes for anions and 5 volumes for amino acids). Homogenates were incubated at 100°C for 2 min, cooled on ice, and subjected to centrifugation (5000*g* for 10 min at 4°C). Anions were measured in the aqueous extracts by anion chromatography with suppressed conductivity detection (Biotronik Co., Maintal, Germany), and amino acids and related compounds were measured with an amino acid analyzer (Biotronik Co.).

For the determination of leaf contents of starch and soluble sugars, rosettes were weighed (0.04 to 0.15 g) and frozen in liquid nitrogen. The leaf material was extracted with perchloric acid, and the debris, containing starch granules, was spun down in a microcentrifuge and washed twice with distilled water. The supernatant, containing soluble intermediates, was neutralized with 3 M Na_2CO_3. For the quantitative solubilization of starch, the debris was incubated in 0.2 M KOH at 95°C for 45 min. The pH of the extract was brought to pH 5.5 with 1 M acetic acid. Starch was degraded to glucose by overnight

incubation in the presence of 70 units of α-amylase and 50 units of amyloglucosidase (in CH_3COONa, pH 4.6). The contents of glucose, fructose, sucrose, and phosphorylated intermediates in neutralized perchloric acid extracts were determined enzymatically according to Stitt et al. (1989).

For metabolite feeding experiments, surface-sterilized seedlings were grown on Murashige and Skoog agar containing 2% sucrose and were supplemented with 1 mM phenylalanine, tryptophan, or tyrosine or with 1 mM each of all three aromatic amino acids.

Rapid Fluorescence Induction Kinetics

The induction kinetics of chlorophyll *a* fluorescence were monitored using the PAM-2000 pulse amplitude modulation fluorometer in the triggered mode. Leaves were dark-adapted for 30 min, F_o and F_m were determined, and leaves were left for an additional 10 min in the dark. Leaves were then illuminated with red light (λ = 600 nm) at a photon flux density of 340 μmol m^{-2} sec^{-1} for 0.8 sec at a resolution of 300 μsec. The proportion of plastoquinone-associated fluorescence was calculated from the ratio $([F_p - F_o] - [F_i - F_o])/(F_p - F_o)$, where F_p is the maximum fluorescence at nonsaturating light and F_i is the fluorescence at the inflection point. The relative abundance of the plastoquinone pool was estimated from the area under the fluorescence induction curves in the absence of Q_A molecules not associated with the plastoquinone pool.

ACKNOWLEDGMENTS

The RNA samples used for the hybridization shown in Figure 5E were provided by Danielle Friedrichsen (Salk Institute), and we thank Gabi Fiene for help with the metabolite feeding experiments. The *cue1-4* allele was a gift from Eric van der Graaff (Institute of Molecular Plant Sciences, Leiden, The Netherlands). We thank our colleagues, in particular Enrique López-Juez, Paul Jarvis, Michael Neff, and Christopher Steele, for many helpful discussions, and we also thank Stephen Mayfield, Marci Surpin, and Rob Larkin for critical reading of the manuscript. We are grateful to the Samuel Roberts Noble Foundation communications department and to Leslie Barden for assistance in preparing figures. This research was supported by U.S. Department of Energy Grant No. ER13993 to J.C., the Deutsche Forschungsgemeinschaft, the Fonds der Chemischen Industrie, the Biotechnology and Biological Sciences Research Council, and a Salk Institute–Samuel Roberts Noble Foundation Fellowship to S.J.S. J.C. is an associate investigator of the Howard Hughes Medical Institute.

Received April 8, 1999; accepted July 6, 1999.

REFERENCES

Anderson, S.L., Teakle, G.R., Martino-Catt, S.J., and Kay, S.A. (1994). Circadian clock– and phytochrome-regulated transcription is conferred by a 78 bp *cis*-acting domain of the Arabidopsis *CAB2* promoter. Plant J. **6,** 457–470.

Aoyama, T., Dong, C.-H., Wu, Y., Carabelli, M., Sessa, G., Ruberti, I., Morelli, G., and Chua, N.-H. (1995). Ectopic expression of the Arabidopsis transcriptional activator *Athb-1* alters leaf cell fate in tobacco. Plant Cell **7,** 1773–1785.

Bagge, P., and Larsson, C. (1986). Biosynthesis of aromatic amino acids by highly purified spinach chloroplasts—Compartmentation and regulation of the reactions. Physiol. Plant. **68,** 641–647.

Chapple, C.C.S., Vogt, T., Ellis, B.E., and Somerville, C.R. (1992). An Arabidopsis mutant defective in the general phenylpropanoid pathway. Plant Cell **4,** 1413–1424.

Chatterjee, M., Sparvoli, S., Edmunds, C., Garosi, P., Findlay, K., and Martin, C. (1996). *DAG*, a gene required for chloroplast differentiation and palisade development in *Antirrhinum majus*. EMBO J. **15,** 4194–4207.

Escoubas, J.-M., Lomas, M., LaRoche, J., and Falkowski, P.G. (1995). Light intensity regulation of *cab* gene transcription is signaled by the redox state of the plastoquinone pool. Proc. Natl. Acad. Sci. USA **92,** 10237–10241.

Fischer, K., Kammerer, B., Gutensohn, M., Arbinger, B., Weber, A., Häusler, R.E., and Flügge, U.-I. (1997). A new class of plastidic phosphate translocators: A putative link between primary and secondary metabolism by the phosphoenolpyruvate/phosphate antiporter. Plant Cell **9,** 453–462.

Flügge, U.-I., Fischer, K., Gross, A., Sebald, W., Lottspeich, F., and Eckerskorn, C. (1989). The triose phosphate-3-phosphoglycerate-phosphate translocator from spinach chloroplasts: Nucleotide sequence of a full-length cDNA clone and import of the in vitro synthesized precursor protein into chloroplasts. EMBO J. **8,** 39–46.

Genty, B., Briantais, J.M., and Baker, N.R. (1989). The relationship between the quantum yield of photosynthetic transport and quenching of chlorophyll fluorescence. Biochim. Biophys. Acta **990,** 87–92.

Horton, P., and Bowyer, J.R. (1990). Chlorophyll fluorescence transients. In Methods in Plant Biochemistry, Vol. 4, J.L. Harwood and J.R. Bowyer, eds (London: Academic Press), pp. 259–296.

Hudson, A., Carpenter, R., Doyle, S., and Coen, E.S. (1993). *Olive*: A key gene required for chlorophyll biosynthesis in *Antirrhinum majus*. EMBO J. **12,** 3711–3719.

Kammerer, B., Fischer, K., Hilpert, B., Schubert, S., Gutensohn, M., Weber, A., and Flügge, U.-I. (1998). Molecular characterization of a carbon transporter in plastids from heterotrophic tissues: The glucose 6-phosphate/phosphate antiporter. Plant Cell **10,** 105–117.

Karpinski, S., Escobar, C., Karpinska, B., Creissen, G., and Mullineaux, P.M. (1997). Photosynthetic electron transport regulates the expression of cytosolic ascorbate peroxidase genes in Arabidopsis during excess light stress. Plant Cell **9,** 627–640.

Karpinski, S., Reynolds, H., Karpinska, B., Wingsle, G., Creissen, G., and Mullineaux, P. (1999). Systemic signaling and acclimation in response to excess excitation energy in Arabidopsis. Science **284,** 654–657.

Kawata, E.E., and Cheung, A.Y. (1990). Molecular analysis of an aurea photosynthetic mutant (*Su/Su*) in tobacco: LHCP depletion leads to pleiotropic mutant phenotypes. EMBO J. **9,** 4197–4203.

Keddie, J.S., Carroll, B., Jones, J.D.G., and Gruissem, W. (1996). The *DCL* gene of tomato is required for chloroplast development and palisade cell morphogenesis in leaves. EMBO J. **15,** 4208–4217.

Kinsman, E.A., and Pyke, K.A. (1998). Bundle sheath cells and cell-specific plastid development in Arabidopsis leaves. Development **125,** 1815–1822.

Krause, G.H., and Weis, E. (1991). Chlorophyll fluorescence and photosynthesis: The basics. Annu. Rev. Plant Physiol. Plant Mol. Biol. **42,** 313–349.

Li, H.-m., Culligan, K., Dixon, R.A., and Chory, J. (1995). *CUE1*: A mesophyll cell–specific positive regulator of light-controlled gene expression in Arabidopsis. Plant Cell **7,** 1599–1610.

Lichtenthaler, H.K., Rohmer, M., and Schwender, J. (1997). Two independent biochemical pathways for isopentenyl diphosphate and isoprenoid biosynthesis in higher plants. Physiol. Plant. **101,** 643–652.

Liu, Y.-G., Mitsukawa, N., Oosumi, T., and Whittier, R.F. (1995). Efficient isolation and mapping of *Arabidopsis thaliana* T-DNA insert junctions by thermal asymmetric interlaced PCR. Plant J. **8,** 457–463.

Loddenkötter, B., Kammerer, B., Fischer, K., and Flügge, U.-I. (1993). Expression of the functional mature chloroplast triose phosphate translocator in yeast internal membranes and purification of the histidine-tagged protein by a single metal-affinity chromatography step. Proc. Natl. Acad. Sci. USA **90,** 2155–2159.

López-Juez, E., Jarvis, R.P., Takeuchi, A., Page, A.M., and Chory, J. (1998). New Arabidopsis *CAB-underexpressed* (*cue*) mutants suggest a close connection between plastid- and phytochrome-regulation of nuclear gene expression. Plant Physiol. **118,** 803–815.

Maxwell, D.P., Laudenbach, D.E., and Huner, N.P.A. (1995). Redox regulation of light-harvesting complex II and *cab* mRNA abundance in *Dunaliella salina*. Plant Physiol. **109,** 787–795.

Neuhaus, H.E., Thom, E., Möhlmann, T., Steup, M., and Kampfenkel, K. (1997). Characterization of a novel eukaryotic ATP/ADP translocator located in the plastid envelope of *Arabidopsis thaliana* L. Plant J. **11,** 73–82.

Norris, S.R., Barrette, T.R., and DellaPenna, D. (1995). Genetic dissection of carotenoid synthesis in Arabidopsis defines plastoquinone as an essential component of phytoene desaturation. Plant Cell **7,** 2139–2149.

Puente, P., Wei, N., and Deng, X.W. (1996). Combinatorial interplay of promoter elements constitutes the minimal determinants for light and developmental control of gene expression in Arabidopsis. EMBO J. **15,** 3732–3743.

Schmid, J., and Amrhein, N. (1995). Molecular organization of the shikimate pathway in higher plants. Phytochemistry **39,** 737–749.

Schreiber, U., Schliwa, U., and Bilger, B. (1986). Continuous recording of photochemical and non-photochemical chlorophyll fluorescence quenching with a new type of modulation fluorometer. Photosynth. Res. **10,** 51–62.

Stitt, M., Lilley, R.M., Gerhardt, R., and Heldt, H.W. (1989). Determination of metabolite levels in specific cells and subcellular compartments of plant leaves. Methods Enzymol. **174,** 518–522.

Tamagnone, L., Merida, A., Parr, A., Mackay, S., Culianez-Macia, F.A., Roberts, K., and Martin, C. (1998a). The AmMYB308 and AmMYB330 transcription factors from Antirrhinum regulate phenylpropanoid and lignin biosynthesis in transgenic tobacco. Plant Cell **10,** 135–154.

Tamagnone, L., Merida, A., Stacey, N., Plaskitt, K., Parr, A., Chang, C.F., Lynn, D., Dow, J.M., Roberts, K., and Martin, C. (1998b). Inhibition of phenolic acid metabolism results in precocious cell death and altered cell morphology in leaves of transgenic tobacco plants. Plant Cell **10,** 1801–1816.

Weber, A., Menzlaff, E., Arbinger, B., Gutensohn, M., Eckerskorn, C., and Flügge, U.-I. (1995). The 2-oxoglutarate/malate translocator of chloroplast envelope membranes: Molecular cloning of a transporter containing a 12-helix motif and expression of the functional protein in yeast cells. Biochemistry **34,** 2621–2627.

Wetzel, C.M., Jiang, C.-Z., Meehan, L.J., Voytas, D.F., and Rodermel, S.R. (1994). Nuclear-organelle interactions: The *immutans* variegation mutant of Arabidopsis is plastid autonomous and impaired in carotenoid biosynthesis. Plant J. **6,** 161–175.